

Exploring Visual Context for Weakly Supervised Person Search

Yichao Yan^{1*}†, Jinpeng Li^{2*}, Shengcai Liao²†, Jie Qin², Bingbing Ni¹, Xiaokang Yang¹, and Ling Shao²

¹ MoE Key Lab of Artificial Intelligence, AI Institute, Shanghai Jiao Tong University, China

² Inception Institute of Artificial Intelligence (IIAI), UAE

{yanyichao91, ljpadam}@gmail.com

Abstract

Person search has recently emerged as a challenging task that jointly addresses pedestrian detection and person re-identification. Existing approaches follow a fully supervised setting where both bounding box and identity annotations are available. However, annotating identities is labor-intensive, limiting the practicability and scalability of current frameworks. This paper inventively considers **weakly supervised person search with only bounding box annotations**. We proposed the first framework to address this novel task, namely *Context-Guided Person Search (CGPS)*, by investigating three levels of context clues (i.e., detection, memory and scene) in unconstrained natural images. The first two are employed to promote local and global discriminative capabilities, while the latter enhances clustering accuracy. Despite its simple design, our CGPS boosts the baseline model by 8.3% in mAP on CUHK-SYSU. Surprisingly, it even achieves comparable performance to two-step person search models, while displaying higher efficiency. Our code is available at <https://github.com/ljpadam/CGPS>.

1. Introduction

Person search [59, 52] aims to retrieve a query person from unconstrained natural images. It therefore needs to simultaneously address the tasks of pedestrian detection and person re-identification (re-id). In contrast to the conventional person re-id task, which requires the pedestrians to be manually cropped or works with an offline detector, the joint detection and re-id paradigm of person search displays higher efficiency in real scenarios. Therefore, person search has recently received increasing attention and emerged as a practical task. Supervised person search in particular has been extensively studied in recent years [37, 51, 4, 55, 42]. Nevertheless, annotating the identities remains labor-intensive. In contrast, relatively accurate

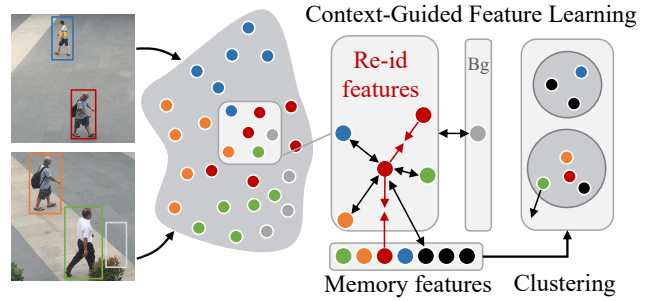


Figure 1: Overall pipeline of the proposed context-guided feature learning framework for weakly supervised person search. We aim to build a framework for person search with only bounding box annotations, where the re-id embeddings are jointly learned with detection. Without identity annotations, initial pseudo labels (colored points) are generated with ImageNet-pretrained weights. We employ the detection context to pull features belonging to the same identity together, while pushing the re-id features of the pedestrians away from the background features. A hard-negative mining strategy is designed to effectively employ the information in the memory. We use the scene context to generate more accurate clustering results.

bounding box annotations could be automatically generated from existing pedestrian detectors [2, 38, 39]. Motivated by this observation and the recent advances in unsupervised person re-id, in this work, we consider person search in the weakly supervised setting, in which there only exist bounding box annotations.

Intuitively, this task can be addressed with a two-step person search model, by first locating the pedestrians with a detector, and then applying an unsupervised person re-id model. However, there are two major issues with this straightforward solution. **1)** Two-step approaches employ two separate models to address pedestrian detection and person re-id, requiring twice as many parameters as one-step models, and introducing high computational overhead. Moreover, these models cannot achieve end-to-end infer-

*indicates equal contributions; † indicates corresponding authors.

ence and are thus inefficient. **2)** As existing unsupervised re-id methods take cropped person images as input, they do not have access to the rich context information when training the detection model, or the scene context. Therefore, directly extending an existing unsupervised person re-id model to address our task without considering the detection and scene context would make the solution suboptimal.

To address the first issue, in this work, we propose the first weakly supervised person search framework, termed as the Context-Guided Person Search Network (**CGPS**). Our model follows the typical architecture of a one-step person search method [52], but it is only supervised with bounding box annotations. To learn re-id features, we adopt similar spirit of an unsupervised re-id model [22], and apply the clustering method to acquire human identities for unsupervised re-id training. This framework naturally inherits the advantages of existing one-step person search models in terms of efficiency, while at the same time avoiding the need for labor-intensive identity annotations.

In terms of the second issue, we further explore the context information for the joint learning framework to pursue discriminative representations for robust unsupervised re-id. Motivated by the recent advances in context learning [15, 58, 26], the following visual context is investigated. **First**, we explore the *detection context* for re-id feature learning. Detection modules, such as Faster-RCNN [44], generate multiple positive predictions associated with each ground truth bounding box, as well as the negative predictions corresponding to the background. We observe that these samples can be naturally employed as a local constraint for learning identity features by keeping the re-id features belonging to the same bounding box close, while pushing the person and background features apart. **Second**, we investigate the global *memory context* to enable the model to pay more attention to hard negative samples in the feature memory. We design a sampling strategy based on the model’s confidence on the negative samples, which adaptively selects the most effective hard negatives. **Third**, we employ the *scene context* to improve the clustering results. Previous methods naively cluster all the re-id features to generate pseudo-labels, without considering the natural context in the scene. We impose an intuitive constraint for clustering, *i.e.*, different people appearing in an image should not belong to the same cluster. We demonstrate that this constraint significantly improves the clustering accuracy. These simple yet effective designs successfully transform an unsupervised person re-id model [22] into a promising weakly supervised person search framework, notably improving the searching performance.

In summary, our contributions are four-fold:

- We propose **the first weakly supervised person search framework**, which extends the current fully supervised paradigm. We expect the pioneering work

to encourage future research in this direction.

- We systematically investigate the visual context clues in the joint learning framework, for both feature learning and clustering. We demonstrate that these context clues work seamlessly in the framework to enhance the re-id feature learning.
- As a one-step person search framework, our model outperforms the two-step models under the same supervision on CUHK-SYSU, while displaying remarkably higher efficiency.
- Our weakly supervised task can be further extended to a **fully unsupervised setting**, requiring neither bounding box nor identity annotations on the target dataset. We believe that the proposed weakly supervised/unsupervised setting complements the conventional supervised one in person search.

2. Related Work

Person Search. Person search is an extension of the person re-id task, which requires pedestrian detection and person re-id to be addressed in uncropped images. Xu *et al.* [54] first introduced this task in 2014, applying a sliding window search strategy with handcrafted features. However, this task did not draw much attention, due to lack of proper benchmarks, until Zheng *et al.* [59] introduced a large dataset for person search, and systematically evaluated different combinations of several pedestrian detectors and re-id models. These became prototypes of two-step person search models. Meanwhile, Xiao *et al.* [52] proposed the first one-step detection and re-id network, enabling end-to-end learning. The follow-up works that have since been introduced can thus be grouped into one-step and two-step models. In general, two-step models [6, 28, 24, 47] pay more attention to the consistency issue, *i.e.*, how to learn discriminative re-id features based on the detection results. In contrast, one-step models [37, 51, 4, 55, 42, 16, 7] focus more on the efficiency issue, *i.e.*, how to design an efficient person search framework.

Despite their impressive progress, all the current models are fully supervised. As it is labor-intensive to annotate all the identities in a large-scale dataset, we explore the weakly supervised setting in this work, *i.e.*, we aim to learn the person search model with only bounding box annotations, while the re-id task is learned in an unsupervised manner.

Unsupervised Person Re-id. Early works, such as ELF [23], LBP [53] and LOMO [31], typically resort to handcrafted features to avoid identity annotation. However, these models only achieve limited performance, and cannot generalize well to large-scale datasets. Deep learning-based methods, on the other hand, can generally be divided into two categories: (1) those that generate pseudo-labels for unsupervised instances [35, 34, 56], and (2) those that translate labeled examples into the unlabeled domain

[50, 46, 60, 20, 21, 40]. For the first category, pseudo-labels are typically generated by clustering the re-id embeddings. If videos are available, temporal constraints [9, 30] can be imposed to improve the precision of the clustering results. The second category is also known as unsupervised domain adaptation. These methods need an annotated source domain for training, and transfers the learned knowledge to the unsupervised target domain. This can be achieved with generative adversarial networks [50, 13, 36, 10, 27], clustering [60, 20, 21, 57], and soft labels assigning [48].

In this work, we consider the task without any re-id annotations. Therefore, we employ clustering to generate pseudo-labels for the re-id task. Furthermore, we extensively explore the context information in the joint learning framework to improve the quality of pseudo-labels and to enhance the discriminative ability of the re-id features.

Learning Visual Context. In addition to annotations, visual data implicitly contains rich context information, which has been widely explored in various vision tasks. For example, the relative location of object parts can be explicitly employed for visual representation learning [15, 43]. Meanwhile, the spatial and semantic relations between objects are helpful for the detection [14, 18, 1] and segmentation [41, 58] tasks. In videos, the spatial-temporal relations can be modeled with a graph model to encode the interactions between objects, and enhance the performance of action recognition [49, 29]. Some person recognition models [26, 55] have also recently employed the social/group context, to pursue robust identity representation.

In our work, we simultaneously investigate three levels of context information, *i.e.*, the detection context, the memory context, and the scene context, and further reveal their importance in weakly supervised person search.

3. Methodology

In this section, we first describe the overall framework for weakly supervised person search (§3.1), and then delve into the details of the proposed context-guided learning strategies (§3.2). Network details are provided in (§3.3).

3.1. Framework Overview

Person Search Framework. In this work, we adopt the typical person search framework [52] which jointly learns detection and re-id in an end-to-end manner. Specifically, this framework is developed upon the Faster-RCNN [44] architecture, as shown in Figure 2(a). Given an input image, the region proposal network (RPN) generates a set of pedestrian proposals, which are subsequently input into an RoI-Align layer to further extract the features of the candidate proposals. The output features are passed to a detection head and a re-id head, respectively. The detection head is trained with a classification loss and a regression loss, which supervise the person/non-person scores, as well

as the bounding box locations. Meanwhile, the re-id head outputs the identity embedding associated with each pedestrian proposal, which is supervised with the pseudo-labels generated in an unsupervised manner.

Unsupervised Person Re-id. Among the recent methods [35, 34, 56, 22] designed for unsupervised re-id, we employ the memory-based loss [22] in our framework, for two reasons. First, it achieves strong performance on several unsupervised person re-id benchmarks, and is more likely to work well in our task. Second, as has been demonstrated in OIM [52], memory-based learning schemes can effectively investigate the information in the unlabeled identities for person search. Specifically, the re-id features of all the training instances are stored in a memory $\mathbf{V} \in \mathbb{R}^{D \times N_a} = \{\mathbf{v}_1, \dots, \mathbf{v}_{N_a}\}$, which contains N_a feature vectors with dimension D , where N_a is the number of instances in the training set. Through clustering, we obtain N_c clusters $\{\mathbb{C}_1, \dots, \mathbb{C}_{N_c}\}$ with centroids $\mathbf{C} \in \mathbb{R}^{D \times N_c} = \{\mathbf{c}_1, \dots, \mathbf{c}_{N_c}\}$. Note that we do not differentiate the clusters containing multiple instances from those with only one (*i.e.*, the unclustered instance). Suppose the network outputs a re-id feature \mathbf{x}_i , the loss is defined as:

$$\mathcal{L}_i = -\log \frac{\exp(\mathbf{x}_i \cdot \mathbf{c}^+ / \tau)}{\sum_{j=1}^{N_c} \exp(\mathbf{x}_i \cdot \mathbf{c}_j / \tau)}, \quad (1)$$

where $\mathbf{c}^+ = \mathbf{c}_j$ if \mathbf{x}_i belongs to the j -th cluster, ‘ \cdot ’ denotes the inner product, and $\tau > 0$ is a temperature hyperparameter that controls the softness of the probability distribution. During backpropagation, the corresponding memory feature is updated by:

$$\mathbf{v} \leftarrow \gamma \mathbf{v} + (1 - \gamma) \mathbf{x}_i, \quad (2)$$

where $\gamma \in [0, 1]$ controls the update ratio in the memory.

3.2. Context-Guided Feature Learning

We observe that the unsupervised re-id model trained with cropped instances does not make full use of the context information in person search. To better adapt the unsupervised re-id to person search, we investigate three types of context information, *i.e.*, the detection context, the memory context, and the scene context.

Detection Context. When training the person search model, the RPN will generate several positive samples for each person, as well as some negative samples corresponding to the background. However, the loss function in Eq. 1 only employs the positive features, which yields two issues. 1) The input re-id features are only compared with memory features, while relations with the intra-batch re-id features are not explored. 2) There is no constraint on the background and foreground features. Although a few supervised person search models [7, 5] have addressed the second issue, the first issue tends to play a more important role in the unsupervised scenario. In this work, we propose a quadruplet loss to simultaneously address both

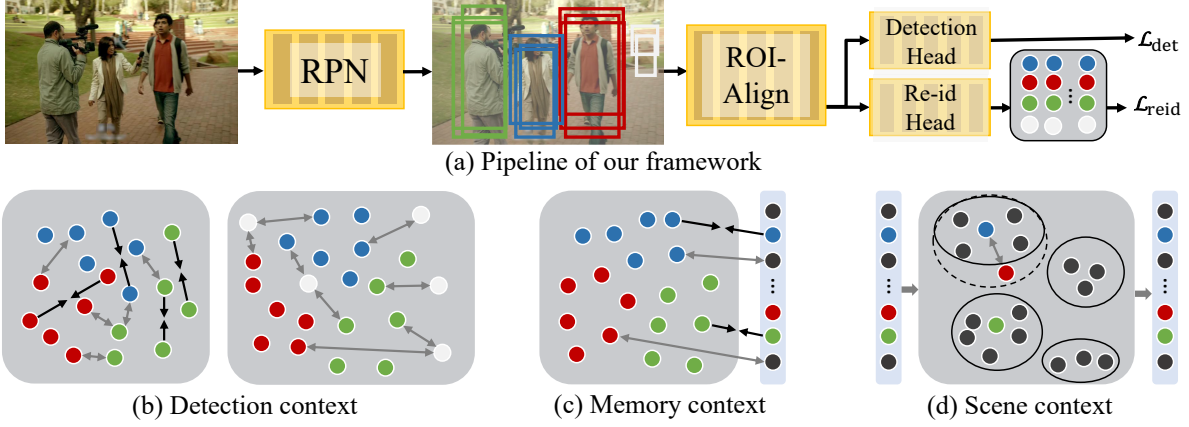


Figure 2: Illustration of our framework. (a) The basic architecture of our framework follows the typical person search model [52], and we employ an unsupervised method [22] to train the re-id branch. (b) We employ the local context information generated by the detection task, to pull positive features belonging to the same instance together, and push background features apart. (c) We sample the hard negatives in the memory to facilitate global feature comparison. (d) Scene context is employed to generate more accurate clustering results.

issues. Specifically, suppose the model outputs n_x re-id features $\mathbf{X} \in \mathbb{R}^{D \times n_x} = \{\mathbf{x}_1, \dots, \mathbf{x}_{n_x}\}$ for the pedestrians, and n_b features corresponding to the backgrounds $\mathbf{B} \in \mathbb{R}^{D \times n_b} = \{\mathbf{b}_1, \dots, \mathbf{b}_{n_b}\}$. For an instance $\mathbf{x}_i \in \mathbf{X}$, the loss function is defined as:

$$\mathcal{L}_i^{\text{DC}} = -\alpha_1 [\min(\mathbf{x}_i \cdot \mathbf{x}^+) - \max(\mathbf{x}_i \cdot \mathbf{x}^-) - m] - \alpha_2 [\min(\mathbf{x}_i \cdot \mathbf{x}) - \max(\mathbf{x}_i \cdot \mathbf{b}) - m], \quad (3)$$

where \mathbf{x}^+ and \mathbf{x}^- denote the positive and negative samples compared with \mathbf{x}_i , $\mathbf{x} \in \mathbf{X}$ and $\mathbf{b} \in \mathbf{B}$, while m denotes the distance margin, and α_1 and α_2 are the weights to balance the two loss terms. As illustrated in Figure 2(b), this function contains two terms. 1) An instance-to-instance term, which pulls the features belonging to the same instance close together, while pushing apart the features of different instances. 2) An instance-to-background term, which pushes the foreground features away from the background features. In this way, we explicitly provide instance-level guidance on the re-id embedding, to yield more discriminative representations.

Memory Context. We observe that the negative samples contribute equally in Eq. 1. However, as indicated by prior works [56, 5], putting more focus on the hard examples plays an important role in improving the model’s discriminative capability. In this work, we explore the hard negative features in the memory, and propose a hard negative sampling strategy by evaluating the cumulative confidence of the hard-negative samples. Without loss of generality, all the negative features are sorted in descending order $\{c_1^-, \dots, c_{N^-}^-\}$ according to their similarities with the input feature, where the number of negative samples is $N^- = N_c - 1$, indicating that the input feature only belongs to one specific cluster. We determine the number of

hardest negative samples with:

$$K = \arg \min_k \left| \frac{\sum_{z=1}^k \mathbf{x}_i \cdot \mathbf{c}_z^-}{\sum_{j=1}^{N^-} \mathbf{x}_i \cdot \mathbf{c}_j^-} - \lambda \right|, \quad (4)$$

where λ is a threshold that controls the ratio of hard negative samples. In this case, Eq. 1 becomes:

$$\mathcal{L}_i^{\text{MC}} = -\log \frac{\exp(\mathbf{x}_i \cdot \mathbf{c}^+ / \tau)}{\exp(\mathbf{x}_i \cdot \mathbf{c}^+ / \tau) + \sum_{k=1}^K \exp(\mathbf{x}_i \cdot \mathbf{c}_k^- / \tau)}. \quad (5)$$

Compared to sampling a fixed size of hard negative samples, our sampling strategy is more flexible to focus on a small set of the most effective negative samples.

The overall loss function is a combination of the targets in Eq. 3 and Eq. 5:

$$\mathcal{L}_{\text{reid}} = \sum_i (\mathcal{L}_i^{\text{DC}} + \mathcal{L}_i^{\text{MC}}). \quad (6)$$

We find these two terms are complementary to each other: $\mathcal{L}_i^{\text{DC}}$ tries to discriminate the local features within a batch, while $\mathcal{L}_i^{\text{MC}}$ focuses more on the global discrimination by comparing the output feature with all the instances in the memory. Therefore, combining them is likely to yield more discriminative representations.

Scene Context. To assign pseudo-labels for the training instances, existing works [22, 8] directly perform clustering (e.g., DBSCAN [19]) on the instance-level re-id features. However, the results of the unsupervised clustering are not perfect, which directly influences the re-id feature learning in the framework. Although some works have tried to improve the clustering reliability with self-paced learning [22] or instance discrimination learning [8], these works only consider regularizing the instance-level representation, neglecting the relative relations between examples in the scene. In this work, we impose a simple constraint on the

Algorithm 1 Clustering with Scene Context

Require: I, V

```
1: Cluster  $V$  with DBSCAN  $\rightarrow \mathbb{C}_1, \dots, \mathbb{C}_{N_c}$ 
2: for  $i \leftarrow 1, \dots, N_c$  do ▷iterate each cluster
3:   for  $j \leftarrow 1, \dots, N_I$  do ▷iterate each image
4:      $\{v_{i,j}^1, \dots, v_{i,j}^K\} \leftarrow \mathbb{C}_i \cap I_j$ 
        ▷find the instances belonging to  $\mathbb{C}_i$  and  $I_j$ 
5:      $l \leftarrow \arg \max_k (v_{i,j}^k \cdot c_i)$ 
        ▷find the instance nearest to the cluster center
6:     for  $k \leftarrow 1, \dots, l-1, l+1, \dots, K$  do
7:        $\mathbb{C}_i \leftarrow \mathbb{C}_i - v_{i,j}^k$  ▷remove this instance from  $\mathbb{C}_i$ 
8:        $N_c \leftarrow N_c + 1$  ▷update the number of clusters
9:        $\mathbb{C}_{N_c} \leftarrow \{v_{i,j}^k\}$  ▷add a new cluster
10:    end for
11:  end for
12: end for
```

clustering results: *the persons appearing in the same image cannot belong to the same cluster*. Specifically, after generating the clustering results based on the memory features, we further go through each cluster and split the clusters containing multiple instances belonging to the same image. For a certain image, only a single instance that is closest to the cluster center will be retained, while other instances will be removed and become unclustered instances. As shown in Figure 2 (d), the original top left cluster contains the blue and red instances. However, since they belong to the same image, the red one, which is far away from the center, is excluded from the cluster. In this way, we are able to generate better clustering results without any additional annotation. Suppose we have N_I training images, and I_i contains the instances in the i -th image. Give $I = \{I_1, \dots, I_{N_I}\}$ and the memory feature V , we summarize the clustering process with scene context in Algorithm 1.

3.3. Network and Implementation Details

We employ ResNet-50 [25] as our backbone, which is divided into two stages following Faster-RCNN [44]. Specifically, the first stage contains the layers from conv1 to conv4, where the features are fed into the RPN to generate a number of region proposals. Then, for each proposal, the RoI-Align layer generates a fixed size ($14 \times 14 \times 1024$) feature map, which is subsequently fed into the second part (conv5 layers) of ResNet-50. Finally, we perform average pooling to the output feature map, resulting in a 2048-dimensional feature vector for each proposal. This vector is then fed into the detection head and the re-id head, respectively. The detection head contains a binary Softmax layer for person/non-person classification, as well as a four-dimensional fully connected layer for bounding box regression. Meanwhile, the re-id head contains a 256-dimensional fully connected layer, and the features are L2 normalized for re-id feature learning.

We initialize the backbone weights with a model pre-trained on ImageNet [12]. The input images are resized to a fixed size of 1000×600 for both training and inference, and we use zero padding to adapt images with different resolutions. Random flipping is applied to the training data as data augmentation. We select the top 300 proposals from RPN. In the training phase, we employ stochastic gradient descent (SGD) as the optimizer, and set the weight decay to 0.0005. We set the batch size to 4 and initialize the learning rate to 0.001, which is reduced by a factor of 10 at epoch 16, training to a total of 22 epochs. We set the default hyperparameters $\gamma = 0.2$, $\alpha_1 = 1$, $\alpha_2 = 0.25$, and $\lambda = 0.7$, and some discussions are given in §4.2. We employ DBSCAN [19] with self-paced training [22] as the clustering method. We set $\epsilon = 0.7$, while other hyperparameters are set to the same values as in SPCL [22]. All the experiments are implemented in Pytorch, with a Tesla V100 GPU.

4. Experiments

4.1. Experimental Setup

Datasets. We evaluate the proposed framework on the following two datasets. **CUHK-SYSU** [52] is one of the largest public datasets designed for person search, which contains 18,184 images captured from streets and TV/movie frames. This dataset also includes 96,143 bounding box annotations, with 8,432 different identities. **PRW** [59] was collected on a university campus from six surveillance cameras. It contains 11,816 video frames, with 43,110 annotated bounding boxes and 932 identities.

Evaluation Protocol. We employ the standard train/test splits for both CUHK-SYSU and PRW. Only the bounding box annotations are employed in the training phase, *i.e.*, 11,216 images with 55,272 bounding boxes for CUHK-SYSU, and 5,705 images with 18,048 boxes for PRW. The test set of CUHK-SYSU contains 2,900 query persons and 6,978 images. It also defines a set of evaluation protocols with different gallery sizes. In the following sections, we report the results with 100 gallery images unless otherwise specified. PRW contains a test set with 2,057 queries and 6,112 images. Following common practice, we report the mean average precision (mAP) and top-1 ranking accuracy as evaluation metrics.

4.2. Analytical Results

Comparative Results. We first evaluate the effectiveness of the proposed context-guided learning strategies. We compare the baseline method (described in §3.1) with different combinations of context information, and report the results on CUHK-SYSU in Table 1. We observe that the baseline framework achieves 65.6% mAP and 68.4% top-1 accuracy without any identity annotation, which builds a strong baseline with SPCL [22]. With the help of detec-

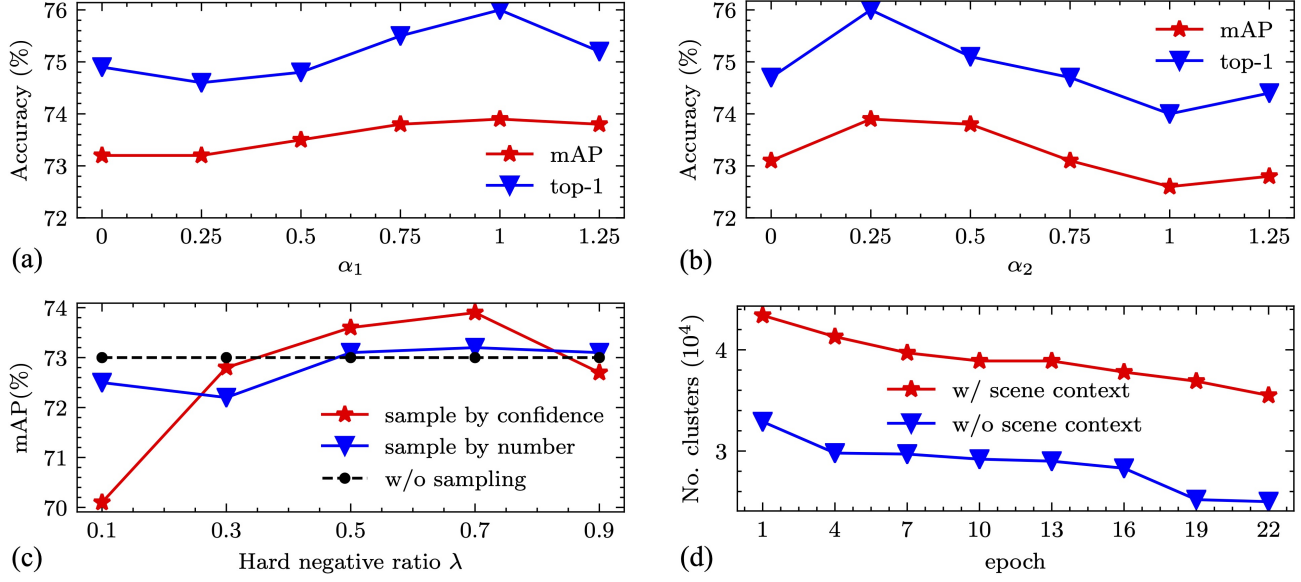


Figure 3: Visualization of the contribution of different types of context clues on CUHK-SYSU. (a) The contribution of the instance-to-instance term in the detection context. (b) The impact of the instance-to-background term in the detection context. (c) The influence of hard negative sampling. (d) The contribution of scene context.

Detection context	Memory context	Scene context	CUHK-SYSU	
			mAP	top-1
			65.6	68.4
✓			69.3 (+3.7)	71.2 (+2.8)
	✓		67.0 (+1.4)	69.3 (+0.9)
		✓	72.3 (+6.7)	74.3 (+5.9)
✓	✓		69.5 (+3.9)	71.7 (+3.3)
✓		✓	73.0 (+7.4)	74.8 (+6.4)
	✓	✓	72.8 (+7.2)	75.0 (+6.6)
✓	✓	✓	73.9 (+8.3)	76.0 (+7.6)

Table 1: Comparative results on CUHK-SYSU when employing different context learning strategies.

Detection context	Memory context	Scene context	PRW	
			mAP	top-1
			10.2	55.1
✓			10.8 (+0.6)	56.5 (+1.4)
	✓		10.6 (+0.4)	57.0 (+1.9)
		✓	11.5 (+1.3)	57.8 (+2.7)
✓	✓	✓	12.5 (+2.3)	58.2 (+3.1)

Table 2: Comparative results on PRW when employing different context learning strategies.

tion, memory and scene context, the model achieves 3.7%, 1.4% and 6.7% improvements in mAP, respectively. Furthermore, by combining these contexts, the model’s performance is further consistently improved. Finally, the model achieves 73.9% mAP when employing all the context, significantly improving the baseline model by **8.3%** in mAP.

The results on PRW are reported in Table 2, where the context information improves the mAP/top-1 accuracy by 2.3%/3.1%. These are less significant compared with the results on CUHK-SYSU. This may be due to the fact that this dataset contains fewer training samples and identities, hence increasing the difficulty of person search.

Detection Context. We visualize the contributions of the instance-to-instance term and instance-to-background term in Figure 3(a) and 3(b), by varying α_1 and α_2 . We observe that both terms play positive roles in re-id feature learning, while the best performance is achieved with $\lambda_1 = 1$ and $\lambda_2 = 0.25$. To differentiate the re-id features of pedestrians from the background, some prior works [59, 7] employ confidence weighted similarity (CWS) for person matching, *i.e.*, multiply the re-id features with the detection confidence. In this work, we employ the instance-to-background term to directly push the two types of features apart, which proves to be effective in our framework.

Memory Context. To evaluate the effectiveness of the memory context, we compare it with the other widely employed “sample by number” strategy, *i.e.*, selecting the top λN^- hardest negatives from all the negative samples. As can be observed from Figure 3(c), our model is sensitive to this hyperparameter. We observe that when $\lambda < 0.3$, the performance significantly decreases as too many easy samples are ignored. However, by selecting a proper hard negative ratio (*i.e.*, $0.5 \sim 0.7$), our proposed strategy achieves notable improvements compared with the “sample by number” strategy, as well as the baseline method without hard negative sampling. These results validate the effectiveness of the hard negatives sampled by our strategy.

Methods		CUHK-SYSU		PRW	
		mAP	top-1	mAP	top-1
fully supervised	OIM [52]	75.5	78.7	21.3	49.4
	DPM+IDE [59]	-	-	20.5	48.3
	IAN [51]	76.3	80.1	23.0	61.9
	NPSM [37]	77.9	81.2	24.2	53.1
	RCAA [4]	79.3	81.3	-	-
	CNN+MGTS [6]	83.0	83.7	32.6	72.1
	CTXG [55]	84.1	86.5	33.4	73.6
	CNN+CLSA [28]	87.2	88.5	38.7	65.0
	QEEPS [42]	88.9	89.1	37.1	76.7
	BINet [16]	90.0	90.7	45.3	81.7
	NAE [7]	91.5	92.4	43.3	80.9
	NAE+ [7]	92.1	92.9	44.0	81.1
	IGPN [17]	90.3	91.4	47.2	87.0
	FPN+RDLR [24]	93.0	94.2	42.9	70.2
	TCTS [47]	93.9	95.1	46.8	87.5
	Our Baseline	81.1	80.6	26.3	59.6
Ours (weakly sup)		73.9	76.0	12.5	58.2

Table 3: Comparison with the state-of-the-art one-step and two-step supervised person search models.

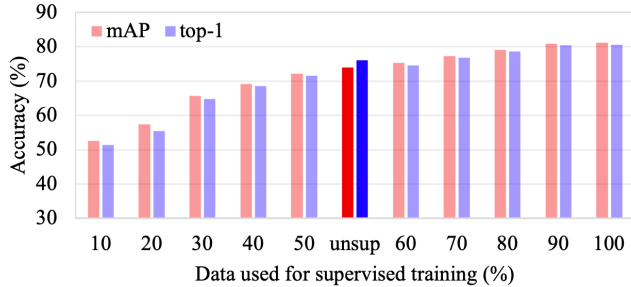


Figure 4: Comparison between our weakly supervised model and the supervised models on CUHK-SYSU.

Scene Context. To reveal how the scene context impacts the clustering results, we visualize the evolution of cluster numbers during training. As shown in Figure 3(d), the number of clusters decreases smoothly, indicating that more and more samples are clustered together. However, there exists a significant gap with and without the scene context constraint, *i.e.*, a large number of (about 10,000) samples are incorrectly clustered at each epoch. We employ the scene context to remove these incompatible samples from the clusters, hence improving the quality of the pseudo-labels. As scene context directly affects the pseudo-labels, we notice that it contributes the most among all the three context clues, demonstrating its importance.

4.3. Comparison with Supervised Models

To further evaluate the performance of our weakly supervised framework, we compare it with the fully supervised models. Our baseline supervised model, *i.e.*, the same struc-

Methods	GFLOPS	Time	mAP	top1
FRCNN + SBL [22]	346	101	67.2	68.9
FRCNN + SPCL[22]	346	100	71.8	72.1
FRCNN + MMT [21]	346	101	73.4	74.9
Ours	281	68	73.9	76.0

Table 4: Comparison with two-step models on CUHK-SYSU, w.r.t. performance and efficiency. SBL denotes the strong baseline in [22]. Runtime is measured by the average inference time in millisecond (ms).

ture as described in §3.1, but assigning all the memory features with ground truth re-id labels, achieves 81.1%/26.3% in mAP on CUHK-SYSU/PRW, respectively. The margins between our unsupervised model and the baseline supervised model are 7.2%/13.8% in mAP, while 4.6%/1.4% in top-1 accuracy. By varying the portion of data utilized during supervised training, we find that our weakly supervised framework achieves comparable performance with supervised models using 50% to 60% annotated samples, as shown in Figure 4. However, compared with the state-of-the-art supervised models, *e.g.*, NAE [7], BINet [16], QEEPS [42], TCTS [47], there still exists a significant margin in performance. We therefore hope this work will provide a starting point to enable future works to explore solutions for bridging this gap.

4.4. Comparison with Two-Step Models

To evaluate the performance and efficiency of the proposed framework, we compare it with several two-step models, which first localize pedestrians with a detector (Faster-RCNN), and then employ an unsupervised re-id method [22, 21] for person retrieval. As can be seen from Table 4, our one-step method not only outperforms the two-step models, but also displays significant advantage in terms of efficiency. Specifically, although our model is based on the re-id training prototype SPCL [22], the context information helps it outperform its two-step counterpart, *i.e.*, 73.9% v.s 71.8% in mAP. For the model complexity and runtime analysis, we employ the same backbone (*i.e.*, ResNet-50) for all the two-step models. Therefore, they obtain similar FLOPS and runtime during inference. As our model only needs a single forward pass to generate both detection results and re-id features, it displays lower FLOPS (346G → 281G) and shorter runtime (101 ms → 68 ms). It is also noteworthy that the parameters of the two-step models are twice as our framework, as they adopt two separate ResNet-50 models for detection and re-id, respectively.

4.5. Further Discussions

In this section, we provide further discussions on the factors that directly impact the performance of our weakly supervised person search model.

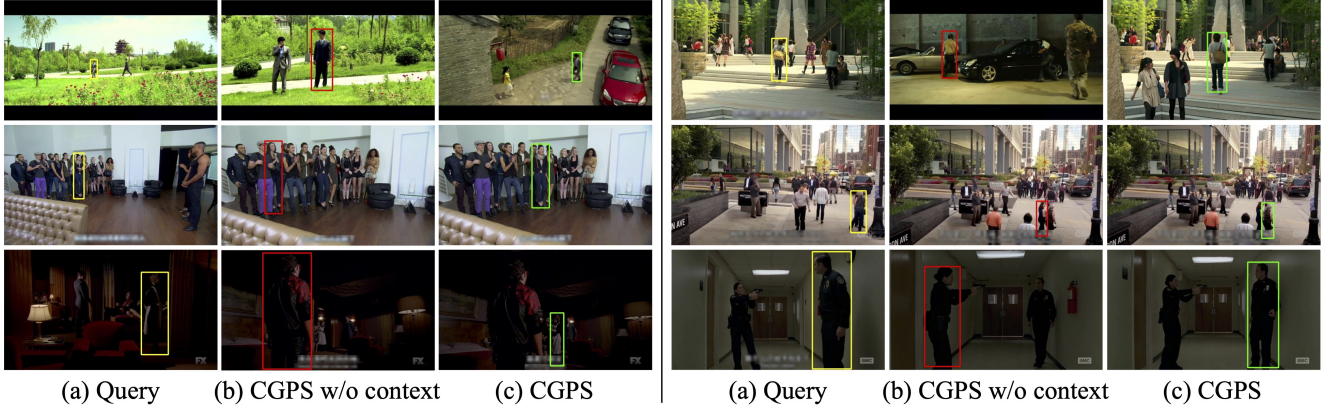


Figure 5: Difficult cases that can be successfully retrieved by CGPS, but not CGPS without context information. The yellow bounding boxes denote the queries, while the green and red ones denote correct and incorrect top-1 matches, respectively.

Methods	GFLOPS	Time	mAP	top1
ResNet-18	146	31	68.5	70.3
ResNet-34	235	40	71.8	73.2
ResNet-50	281	68	73.9	76.0
ResNet-101	327	81	74.2	76.1

Table 5: Results on CUHK-SYSU with various backbones.

Input Size	GFLOPS	Time	mAP	top1
800×480	259	66	70.8	73.1
1000×600	281	68	73.9	76.0
1200×720	307	76	74.1	75.7
1400×840	339	83	74.5	76.8
1600×960	374	88	75.0	77.1

Table 6: Results on CUHK-SYSU with different input sizes.

Different Backbones. We first analyze the influence of different backbone networks in our weakly supervised setting, by employing different structures from the ResNet family. As shown in Table 5, using different backbones considerably affects our model’s performance. With ResNet-18, the model achieves 68.5% in mAP, while its performance is significantly improved to 74.2% when employing ResNet-101. However, deeper backbone networks also bring significantly higher FLOPS (146G \rightarrow 327G) and longer runtime (31 ms \rightarrow 81 ms). In practice, a suitable backbone needs to be carefully selected to meet the requirements of real-world applications.

Input Image Size. As shown in Table 6, we also find positive correlation between the model’s performance and the input size. Specifically, enlarging the input size from 800×480 to 1000×600 leads to a performance gain of 3.1% in mAP. However, continuing to increase the input size only yields marginal improvements, while introducing a large computational overhead. Therefore, the input size of 1000×600 achieves a good trade-off between performance

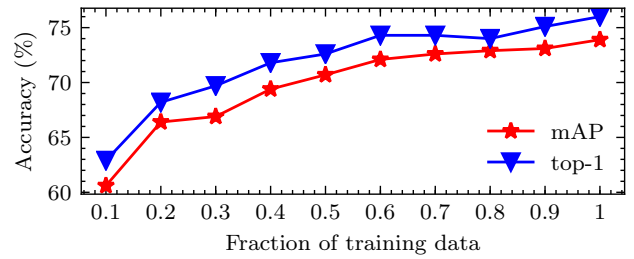


Figure 6: Results on CUHK-SYSU with different numbers of samples for weakly supervised training.

and efficiency in our framework.

Training Samples. In Figure 6, we illustrate the impact of different numbers of training samples on the weakly supervised person search task. We observe that more training samples generate better results. Therefore, in the future, we can collect more weakly annotated data to further enhance the performance of our model. More discussions are made on this point in the supplementary material.

4.6. Qualitative Results

We visualize some qualitative results in Figure 5. As can be observed, our model successfully retrieves the target person in several challenging cases, where the baseline model without the guidance of context information fails. As can be seen from the top-left example, CGPS retrieves the correct target from a different viewpoint. In contrast, the baseline model returns another person with similar appearance. Other examples also show that our context-guided model is more robust to the situations of occlusion, as well as illumination/scale variations. These results demonstrate the importance of the context clues in our framework.

4.7. Training Data Combinations

To further reveal the impacts of combining different training data, we employ different configurations of CUHK-

Training Data			CUHK-SYSU		PRW	
CUHK	PRW	COCO	mAP	top-1	mAP	top-1
✓			73.9	76.0	11.1	57.0
	✓		47.8	50.0	12.5	58.2
✓	✓		74.1	76.0	13.7	62.3
✓		✓	71.4	73.8	10.7	58.8
	✓	✓	65.1	67.0	12.8	61.8
✓	✓	✓	70.4	72.9	13.1	65.3

Table 7: Comparative results on CUHK-SYSU and PRW when employing different combinations of training data.

Annotation	CUHK-SYSU		PRW	
	mAP	top-1	mAP	top-1
Cascade R-CNN [3]	69.0	70.9	11.5	56.6
RetinaNet [32]	69.7	72.0	11.3	55.0
EMD+RM [11]	70.1	72.3	11.9	58.7
GT	73.9	76.0	12.5	58.2

Table 8: Comparative results on CUHK-SYSU and PRW when employing different bounding box annotations.

SYSU, PRW, and an external dataset COCO [33] for training. Specifically, we select 6,500 images containing pedestrians from the original COCO dataset, and only utilize pedestrian bounding box annotations. As shown in Table 7, the combination of CUHK-SYSU and PRW achieves the best performance on both datasets. Furthermore, the improvement on PRW is more significant, maybe due to the fact that PRW contains fewer training samples. However, adding more training data does not always bring improvement, *e.g.*, the combination of CUHK-SYSU and COCO achieves inferior performance compared with employing CUHK-SYSU alone. This is because of the domain gaps between these datasets; therefore, considering domain adaptation is another direction worth exploration in the future.

4.8. Extension to Unsupervised Person Search

Our weakly supervised framework can be naturally extended to a fully unsupervised setting by generating the bounding box annotations from existing pedestrian detectors. We compare the model trained with the ground-truth (GT) bounding boxes and the generated/predicted ones from several pedestrian detectors trained on *CrowdHuman* [45]. The comparison results are reported in Table 8. We observe that no matter which detector is employed, we can obtain satisfactory performance on both datasets, which is only slightly lower compared with the models trained with GT bounding boxes. This shows the potential of building a person search framework completely free of manual annotations.

5. Conclusion

This paper introduces a new research direction for person search, *i.e.*, weakly supervised person search, to address the task with only bounding box locations, avoiding the need to collect labor-intensive identity annotations. We propose to address the task by taking advantage of the efficient one-step person search framework, as well as unsupervised re-id models. By extensively exploring the detection, memory, and scene context, we successfully develop a weakly supervised person search framework. Our framework achieves promising results on two benchmarks, but there still exists a significant gap compared with fully supervised models. Considering the great advances in weakly supervised and unsupervised learning in recent years, we expect that this work will foster future research towards solving this.

References

- [1] Ehud Barnea and Ohad Ben-Shahar. Exploring the bounds of the utility of context for object detection. In *IEEE Conf. Comput. Vis. Pattern Recog.*, pages 7412–7420, 2019. 3
- [2] Garrick Brazil, Xi Yin, and Xiaoming Liu. Illuminating pedestrians via simultaneous detection and segmentation. In *Int. Conf. Comput. Vis.*, pages 4960–4969, 2017. 1
- [3] Zhaowei Cai and Nuno Vasconcelos. Cascade R-CNN: delving into high quality object detection. In *IEEE Conf. Comput. Vis. Pattern Recog.*, pages 6154–6162, 2018. 9
- [4] Xiaojun Chang, Po-Yao Huang, Yi-Dong Shen, Xiaodan Liang, Yi Yang, and Alexander G. Hauptmann. RCAA: relational context-aware agents for person search. In *Eur. Conf. Comput. Vis.*, pages 86–102, 2018. 1, 2, 7
- [5] Di Chen, Shanshan Zhang, Wanli Ouyang, Jian Yang, and Bernt Schiele. Hierarchical online instance matching for person search. In *AAAI*, pages 10518–10525, 2020. 3, 4
- [6] Di Chen, Shanshan Zhang, Wanli Ouyang, Jian Yang, and Ying Tai. Person search via a mask-guided two-stream CNN model. In *Eur. Conf. Comput. Vis.*, pages 764–781, 2018. 2, 7
- [7] Di Chen, Shanshan Zhang, Jian Yang, and Bernt Schiele. Norm-aware embedding for efficient person search. In *IEEE Conf. Comput. Vis. Pattern Recog.*, pages 12612–12621, 2020. 2, 3, 6, 7
- [8] Guangyi Chen, Yuhao Lu, Jiwen Lu, and Jie Zhou. Deep credible metric learning for unsupervised domain adaptation person re-identification. In *Eur. Conf. Comput. Vis.*, pages 643–659, 2020. 4
- [9] Yanbei Chen, Xiatian Zhu, and Shaogang Gong. Deep association learning for unsupervised video person re-identification. In *Brit. Mach. Vis. Conf.*, page 48, 2018. 3
- [10] Yanbei Chen, Xiatian Zhu, and Shaogang Gong. Instance-guided context rendering for cross-domain person re-identification. In *Int. Conf. Comput. Vis.*, pages 232–242, 2019. 3
- [11] Xuangeng Chu, Anlin Zheng, Xiangyu Zhang, and Jian Sun. Detection in crowded scenes: One proposal, multiple pre-

- dictionaries. In *IEEE Conf. Comput. Vis. Pattern Recog.*, pages 12211–12220, 2020. [9](#)
- [12] Jia Deng, Wei Dong, Richard Socher, Li-Jia Li, Kai Li, and Fei-Fei Li. Imagenet: A large-scale hierarchical image database. In *IEEE Conf. Comput. Vis. Pattern Recog.*, pages 248–255, 2009. [5](#)
- [13] Weijian Deng, Liang Zheng, Qixiang Ye, Guoliang Kang, Yi Yang, and Jianbin Jiao. Image-image domain adaptation with preserved self-similarity and domain-dissimilarity for person re-identification. In *IEEE Conf. Comput. Vis. Pattern Recog.*, pages 994–1003, 2018. [3](#)
- [14] Santosh Kumar Divvala, Derek Hoiem, James Hays, Alexei A. Efros, and Martial Hebert. An empirical study of context in object detection. In *IEEE Conf. Comput. Vis. Pattern Recog.*, pages 1271–1278, 2009. [3](#)
- [15] Carl Doersch, Abhinav Gupta, and Alexei A. Efros. Unsupervised visual representation learning by context prediction. In *Int. Conf. Comput. Vis.*, pages 1422–1430, 2015. [2, 3](#)
- [16] Wenkai Dong, Zhaoxiang Zhang, Chunfeng Song, and Tieniu Tan. Bi-directional interaction network for person search. In *IEEE Conf. Comput. Vis. Pattern Recog.*, pages 2836–2845, 2020. [2, 7](#)
- [17] Wenkai Dong, Zhaoxiang Zhang, Chunfeng Song, and Tieniu Tan. Instance guided proposal network for person search. In *IEEE Conf. Comput. Vis. Pattern Recog.*, pages 2582–2591, 2020. [7](#)
- [18] Nikita Dvornik, Julien Mairal, and Cordelia Schmid. Modeling visual context is key to augmenting object detection datasets. In *Eur. Conf. Comput. Vis.*, pages 375–391, 2018. [3](#)
- [19] Martin Ester, Hans-Peter Kriegel, Jörg Sander, and Xiaowei Xu. A density-based algorithm for discovering clusters in large spatial databases with noise. In *International Conference on Knowledge Discovery and Data Mining*, pages 226–231, 1996. [4, 5](#)
- [20] Yang Fu, Yunchao Wei, Guanshuo Wang, Yuqian Zhou, Honghui Shi, and Thomas S. Huang. Self-similarity grouping: A simple unsupervised cross domain adaptation approach for person re-identification. In *Int. Conf. Comput. Vis.*, pages 6111–6120, 2019. [3](#)
- [21] Yixiao Ge, Dapeng Chen, and Hongsheng Li. Mutual mean-teaching: Pseudo label refinery for unsupervised domain adaptation on person re-identification. In *International Conference on Learning Representations*, 2020. [3, 7](#)
- [22] Yixiao Ge, Feng Zhu, Dapeng Chen, Rui Zhao, and Hongsheng Li. Self-paced contrastive learning with hybrid memory for domain adaptive object re-id. In *Adv. Neural Inform. Process. Syst.*, 2020. [2, 3, 4, 5, 7](#)
- [23] Douglas Gray and Hai Tao. Viewpoint invariant pedestrian recognition with an ensemble of localized features. In *Eur. Conf. Comput. Vis.*, pages 262–275, 2008. [2](#)
- [24] Chuchu Han, Jiacheng Ye, Yunshan Zhong, Xin Tan, Chi Zhang, Changxin Gao, and Nong Sang. Re-id driven localization refinement for person search. In *Int. Conf. Comput. Vis.*, pages 9813–9822, 2019. [2, 7](#)
- [25] Kaiming He, Xiangyu Zhang, Shaoqing Ren, and Jian Sun. Deep residual learning for image recognition. In *IEEE Conf. Comput. Vis. Pattern Recog.*, pages 770–778, 2016. [5](#)
- [26] Qingqiu Huang, Yu Xiong, and Dahua Lin. Unifying identification and context learning for person recognition. In *IEEE Conf. Comput. Vis. Pattern Recog.*, pages 2217–2225, 2018. [2, 3](#)
- [27] Yan Huang, Qiang Wu, Jingsong Xu, and Yi Zhong. SBS-GAN: suppression of inter-domain background shift for person re-identification. In *Int. Conf. Comput. Vis.*, pages 9526–9535, 2019. [3](#)
- [28] Xu Lan, Xiatian Zhu, and Shaogang Gong. Person search by multi-scale matching. In *Eur. Conf. Comput. Vis.*, volume 11205, pages 553–569, 2018. [2, 7](#)
- [29] Maosen Li, Siheng Chen, Xu Chen, Ya Zhang, Yanfeng Wang, and Qi Tian. Actional-structural graph convolutional networks for skeleton-based action recognition. In *IEEE Conf. Comput. Vis. Pattern Recog.*, pages 3595–3603, 2019. [3](#)
- [30] Minxian Li, Xiatian Zhu, and Shaogang Gong. Unsupervised tracklet person re-identification. *IEEE Trans. Pattern Anal. Mach. Intell.*, 42(7):1770–1782, 2020. [3](#)
- [31] Shengcai Liao, Yang Hu, Xiangyu Zhu, and Stan Z. Li. Person re-identification by local maximal occurrence representation and metric learning. In *IEEE Conf. Comput. Vis. Pattern Recog.*, pages 2197–2206, 2015. [2](#)
- [32] Tsung-Yi Lin, Priya Goyal, Ross B. Girshick, Kaiming He, and Piotr Dollár. Focal loss for dense object detection. In *Int. Conf. Comput. Vis.*, pages 2999–3007, 2017. [9](#)
- [33] Tsung-Yi Lin, Michael Maire, Serge J. Belongie, James Hays, Pietro Perona, Deva Ramanan, Piotr Dollár, and C. Lawrence Zitnick. Microsoft COCO: common objects in context. In *Eur. Conf. Comput. Vis.*, pages 740–755, 2014. [9](#)
- [34] Yutian Lin, Xuanyi Dong, Liang Zheng, Yan Yan, and Yi Yang. A bottom-up clustering approach to unsupervised person re-identification. In *AAAI*, pages 8738–8745, 2019. [2, 3](#)
- [35] Yutian Lin, Lingxi Xie, Yu Wu, Chenggang Yan, and Qi Tian. Unsupervised person re-identification via softened similarity learning. In *IEEE Conf. Comput. Vis. Pattern Recog.*, pages 3387–3396, 2020. [2, 3](#)
- [36] Chong Liu, Xiaojun Chang, and Yi-Dong Shen. Unity style transfer for person re-identification. In *IEEE Conf. Comput. Vis. Pattern Recog.*, pages 6886–6895, 2020. [3](#)
- [37] Hao Liu, Jiashi Feng, Zequn Jie, Jayashree Karlekar, Bo Zhao, Meibin Qi, Jianguo Jiang, and Shuicheng Yan. Neural person search machines. In *Int. Conf. Comput. Vis.*, pages 493–501, 2017. [1, 2, 7](#)
- [38] Wei Liu, Shengcai Liao, Weidong Hu, Xuezhi Liang, and Xiao Chen. Learning efficient single-stage pedestrian detectors by asymptotic localization fitting. In *Eur. Conf. Comput. Vis.*, pages 643–659, 2018. [1](#)
- [39] Wei Liu, Shengcai Liao, Weiqiang Ren, Weidong Hu, and Yinan Yu. High-level semantic feature detection: A new perspective for pedestrian detection. In *IEEE Conf. Comput. Vis. Pattern Recog.*, pages 5187–5196, 2019. [1](#)
- [40] Djebri Mekhazni, Amran Bhuiyan, George S. Eskander, Ekladios, and Eric Granger. Unsupervised domain adaptation in the dissimilarity space for person re-identification. In *Eur. Conf. Comput. Vis.*, pages 159–174, 2020. [3](#)

- [41] Roozbeh Mottaghi, Xianjie Chen, Xiaobai Liu, Nam-Gyu Cho, Seong-Whan Lee, Sanja Fidler, Raquel Urtasun, and Alan L. Yuille. The role of context for object detection and semantic segmentation in the wild. In *IEEE Conf. Comput. Vis. Pattern Recog.*, pages 891–898, 2014. [3](#)
- [42] Bharti Munjal, Sikandar Amin, Federico Tombari, and Fabio Galasso. Query-guided end-to-end person search. In *IEEE Conf. Comput. Vis. Pattern Recog.*, pages 811–820, 2019. [1](#), [2](#), [7](#)
- [43] Mehdi Noroozi and Paolo Favaro. Unsupervised learning of visual representations by solving jigsaw puzzles. In *Eur. Conf. Comput. Vis.*, pages 69–84, 2016. [3](#)
- [44] Shaoqing Ren, Kaiming He, Ross B. Girshick, and Jian Sun. Faster R-CNN: towards real-time object detection with region proposal networks. *IEEE Trans. Pattern Anal. Mach. Intell.*, pages 1137–1149, 2017. [2](#), [3](#), [5](#)
- [45] Shuai Shao, Zijian Zhao, Boxun Li, Tete Xiao, Gang Yu, Xiangyu Zhang, and Jian Sun. Crowdhuman: A benchmark for detecting human in a crowd. *CoRR*, abs/1805.00123, 2018. [9](#)
- [46] Jifei Song, Yongxin Yang, Yi-Zhe Song, Tao Xiang, and Timothy M. Hospedales. Generalizable person re-identification by domain-invariant mapping network. In *IEEE Conf. Comput. Vis. Pattern Recog.*, pages 719–728, 2019. [3](#)
- [47] Cheng Wang, Bingpeng Ma, Hong Chang, Shiguang Shan, and Xilin Chen. TCTS: A task-consistent two-stage framework for person search. In *IEEE Conf. Comput. Vis. Pattern Recog.*, pages 11949–11958, 2020. [2](#), [7](#)
- [48] Dongkai Wang and Shiliang Zhang. Unsupervised person re-identification via multi-label classification. In *IEEE Conf. Comput. Vis. Pattern Recog.*, pages 10978–10987, 2020. [3](#)
- [49] Xiaolong Wang and Abhinav Gupta. Videos as space-time region graphs. In *Eur. Conf. Comput. Vis.*, pages 413–431, 2018. [3](#)
- [50] Longhui Wei, Shiliang Zhang, Wen Gao, and Qi Tian. Person transfer GAN to bridge domain gap for person re-identification. In *IEEE Conf. Comput. Vis. Pattern Recog.*, pages 79–88, 2018. [3](#)
- [51] Jimin Xiao, Yanchun Xie, Tammam Tillo, Kaizhu Huang, Yunchao Wei, and Jiashi Feng. IAN: the individual aggregation network for person search. *Pattern Recognit.*, 87:332–340, 2019. [1](#), [2](#), [7](#)
- [52] Tong Xiao, Shuang Li, Bochao Wang, Liang Lin, and Xiaogang Wang. Joint detection and identification feature learning for person search. In *IEEE Conf. Comput. Vis. Pattern Recog.*, pages 3376–3385, 2017. [1](#), [2](#), [3](#), [4](#), [5](#), [7](#)
- [53] Fei Xiong, Mengran Gou, Octavia I. Camps, and Mario Sznajder. Person re-identification using kernel-based metric learning methods. In *Eur. Conf. Comput. Vis.*, pages 1–16, 2014. [2](#)
- [54] Yuanlu Xu, Bingpeng Ma, Rui Huang, and Liang Lin. Person search in a scene by jointly modeling people commonness and person uniqueness. In *ACM Int. Conf. Multimedia*, pages 937–940, 2014. [2](#)
- [55] Yichao Yan, Qiang Zhang, Bingbing Ni, Wendong Zhang, Minghao Xu, and Xiaokang Yang. Learning context graph for person search. In *IEEE Conf. Comput. Vis. Pattern Recog.*, pages 2158–2167, 2019. [1](#), [2](#), [3](#), [7](#)
- [56] Kaiwei Zeng, Munan Ning, Yaohua Wang, and Yang Guo. Hierarchical clustering with hard-batch triplet loss for person re-identification. In *IEEE Conf. Comput. Vis. Pattern Recog.*, pages 13654–13662, 2020. [2](#), [3](#), [4](#)
- [57] Yunpeng Zhai, Shijian Lu, Qixiang Ye, Xuebo Shan, Jie Chen, Rongrong Ji, and Yonghong Tian. Ad-cluster: Augmented discriminative clustering for domain adaptive person re-identification. In *IEEE Conf. Comput. Vis. Pattern Recog.*, pages 9018–9027, 2020. [3](#)
- [58] Hang Zhang, Kristin J. Dana, Jianping Shi, Zhongyue Zhang, Xiaogang Wang, Amrith Tyagi, and Amit Agrawal. Context encoding for semantic segmentation. In *IEEE Conf. Comput. Vis. Pattern Recog.*, pages 7151–7160, 2018. [2](#), [3](#)
- [59] Liang Zheng, Hengheng Zhang, Shaoyan Sun, Manmohan Chandraker, Yi Yang, and Qi Tian. Person re-identification in the wild. In *IEEE Conf. Comput. Vis. Pattern Recog.*, pages 3346–3355, 2017. [1](#), [2](#), [5](#), [6](#), [7](#)
- [60] Zhun Zhong, Liang Zheng, Zhiming Luo, Shaozi Li, and Yi Yang. Invariance matters: Exemplar memory for domain adaptive person re-identification. In *IEEE Conf. Comput. Vis. Pattern Recog.*, pages 598–607, 2019. [3](#)